Trans Indian Inst Met (2019) 72(4):889–898
https://doi.org/10.1007/s12666-018-1547-x

TECHNICAL PAPER

Numerical Analysis of Turbulence Inhibitor Toward Inclusion Separation Efficiency in Tundish

Rishikesh Mishra[1] · **Dipak Mazumdar**[1]

Received: 11 July 2018 / Accepted: 17 December 2018 / Published online: 5 January 2019

Abstract There is scientific agreement on tundish performance improvement on incorporating a turbulence inhibitor box or turbostop, but also a dearth of commentary on the principles of its design. Industrial practice often employs incredible detail and customization into these devices, in parts due to this lack of perspective. In the current work, numerical simulation has been carried out to examine the elements of turbostop design, in context of modifying flow to promote inclusion removal in the tundish. Isothermal turbulent single-phase steady-state analysis was carried out to study the residence time distribution in aqueous tundish systems and analyze the effect of turbostop design on it. Significant improvement in bulk flow characteristics was found with the use of tapered walls and such device shapes which adhere closely to local flow symmetry near the shroud. Additional elements such as ridged walls and partial cover were found to have small impact on overall flow characteristics. More generally, the efficiency of turbulence containment is predominantly a function of local flow redirection around the submerged jet, rather than specific to bulk tundish design, which shows nominal sensitivity to local flow behavior in the containment region.

Keywords Residence time distribution · Turbulence inhibition · Inclusion flotation · Flow control · Design analysis

✉ Rishikesh Mishra
mrishi@iitk.ac.in

[1] Department of Materials Science and Engineering, Indian Institute of Technology Kanpur, Kanpur 208016, India

1 Introduction

Typical objectives of tundish are inclusion separation, thermochemical modification and homogenization, and reducing exposure of bulk volume to thermal and compositional shock during grade transitions or ladle changeover, thus ensuring efficient operation of downstream casting assembly. In order to ensure fine degree of control over composition and cleanliness of solidification product, flow control devices (FCDs) such as weir, dam and pouring box are frequently inlayed in tundishes to influence bulk flow characteristics to favor inclusion removal.

Operational agenda and factors like inclusion distribution and throughput rate heavily influence decisions regarding flow modification. However, speaking generally, a good assessment of inclusion removal efficiency, especially for larger size inclusions (40 microns or greater) [1], can be found through the analysis of Residence Time Distribution (RTD), which characterize flow and mixing in a tundish [1]. In a related study by the current authors, a good correspondence has been observed between the two for water model as well as industrial systems [2].

Defined as the time spent by an incoming fluid element in the tundish volume, the frequency distribution of residence time can be obtained by injecting tracer at the inlet (continuously or as a pulse) and tracking it at the outlet [1]. The key parameters which characterize the 'C-curves' so obtained are, namely the minimum breakthrough time, t_{min} (normalized as θ_{min}), when the tracer concentration is first detected at the outlet; time to attain peak tracer concentration, t_{peak} (or θ_{peak}); and t_{av} (or θ_{av}), the mean residence time for the distribution:

$$\theta_{av} = \frac{1}{\tau}\frac{\int_0^{2\tau} Ctdt}{\int_0^{2\tau} Cdt} \quad (1)$$

C is a characteristic property proportional to tracer concentration and τ is the theoretical average/nominal residence time for an unskewed distribution, defined as

$$\text{Nominal residence time, } \tau = \frac{\text{Volume of vessel}}{\text{Volumetric flow rate}} \quad (2)$$

Fractional volumes in the tundish exhibiting different flow characteristics have been found to correlate with the RTD parameters [3], viz.

$$\text{Dead volume, } V_d = 1 - \frac{Q_a}{Q}\theta_{av} \quad (3)$$

$$\text{Dispersed plug volume, } V_{dp} = \frac{\theta_{min} + \theta_{peak}}{2} \quad (4)$$

$$\text{Well mixed volume, } V_m = 1 - (V_d + V_{dp}) \quad (5)$$

where Q_a/Q represents the fraction of flow through active region of the tundish [2, 4]. Small dead volume and larger fraction of quiescent dispersed plug flow are considered conducive for inclusion flotation, a dominant separation pathway for larger inclusion size [1, 2]. The highly turbulent gas–liquid plunging jet from ladle shroud wields a negative influence on the same. Consequently, the turbulent stream is confined to the inlet zone by the use of pouring boxes and turbulence inhibitor, or 'turbostop,' to shield the bulk flow from its influence. The stream is instead redirected toward the surface, preventing short-circuiting and premature inclusion transport [4], while also increasing exposure of inclusion carrying steel with the slag layer [5].

Although a variety of turbostop designs are reported in scientific investigations on flow control [4–8], incorporating square [4, 5], circular [6] and octagonal structure [7] with solid, perforated or slotted walls [7], the focus has primarily been on dams, weirs and baffles to influence the bulk flow. Investigations on FCD configuration have reported that the presence of turbostop leads to substantial improvement in the flow [8, 9]. However, a lack of comprehensive evaluation of its design has resulted in the employment of myriad designs in the industrial practice [10–12]. The present study attempts to address this by a CFD based approach to model flow physics in the tundish, understand the working principle of the device and evaluate the performance of tundish–turbostop geometry couplings.

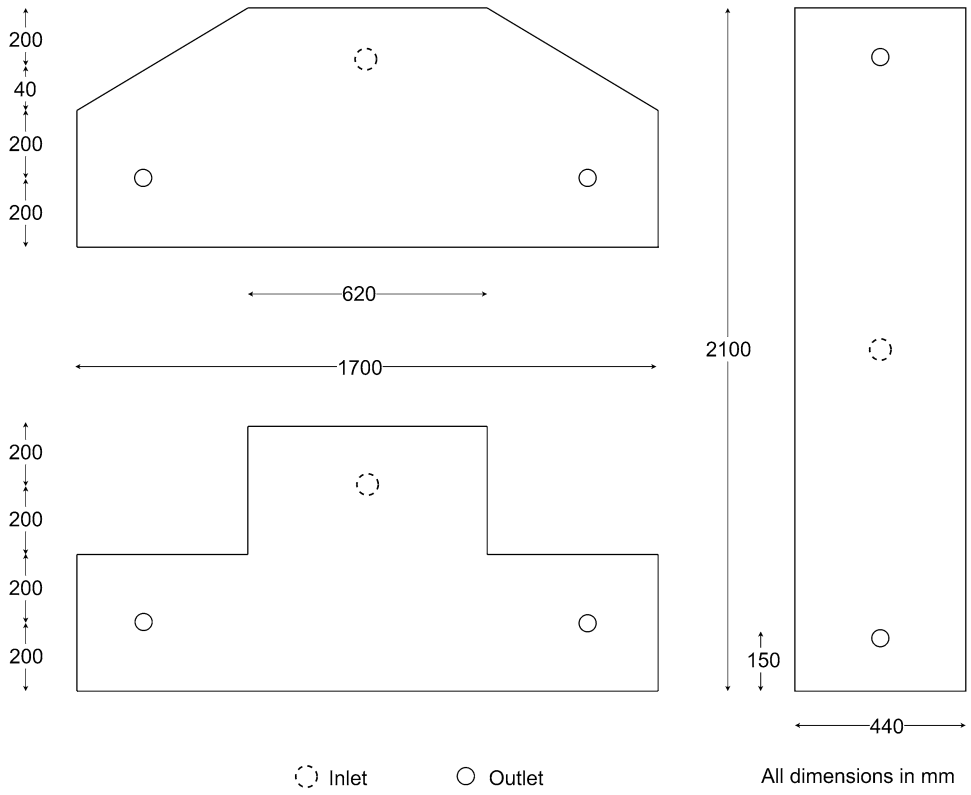

Fig. 1 Layout of reservoir designs: (clockwise from top) delta-, rectangular- and T-shaped reservoir

Table 1 Process parameters

Reservoir	Delta	T shaped	Rectangular
Reservoir volume	0.88 m^3	0.874 m^3	0.872 m^3
Nominal residence time	293.32 s	291.32 s	290.67 s
Side wall inclination	10° outward		
Operating bath height	700 mm		
Shroud submergence depth	150 mm		
Shroud (inlet) diameter	70 mm		
Outlet diameter	22 mm		
Ambience	NTP (298 K, 1 atm)		
Working fluid	Water		
Tracer	Water		
Flow rate	90 l/min (1.5 kg/s)		
Density	998.1 kg/m^3		
Dynamic viscosity	1.03 mPa		
Mass diffusivity	2.88e−05 m^2/s		

Table 2 Nomenclature used to identify elements of turbostop design

First letter	Second letter	Third letter (optional)
V Vertical wall	R Rectangular (square) shape	s slots near the bottom of device walls
T Tapered wall (10° outward from vertical)	C Circular shape	c partially covered top blocking approximately 50% area of opening
	S Similar shape as the bulk geometry	r three regularly spaced ridges projecting from the inner walls

2 Present Study

2.1 Mathematical Modeling

With the exception of initial filling, final emptying and intermittent periods of ladle changeover, the tundish is operated at a fluctuating but nearly constant height (operating bath height). The flow in these prolonged periods exhibits a quasi-steady-state behavior and can be modeled as such with reasonable accuracy [2]. It is also notable that excluding the inlet region, flow in a real tundish is only transitionally turbulent [1]. Coupled with multiphase interactions of steel, slag and gas, this adds enormous physical complexity and mathematical limitations for accurate numerical approximation of steady state. Nevertheless, a reasonably practical approximation of tundish flow has been found in modeling the behavior as a fully turbulent single-phase steady state [2, 13].

With these approximations, a RANS-based approach was adopted to establish a three-dimensional steady isothermal single-phase flow in water model tundish using the standard k–ε model for turbulence [14]. The governing equations of fluid flow and turbulence can be expressed as:

$$\frac{\partial u_i}{\partial x_i} = 0 \tag{6}$$

$$\rho \frac{\partial (u_i u_j)}{\partial x_j} = -\frac{\partial p}{\partial x_i} + \frac{\partial}{\partial x_j}\left(\mu_{\text{eff}} \frac{\partial u_i}{\partial x_j}\right) + \rho g_i \tag{7}$$

$$\frac{\partial \rho k u_i}{\partial x_i} = \frac{\partial}{\partial x_j}\left(\frac{\mu_t}{\sigma_k}\frac{\partial k}{\partial x_j}\right) + 2\mu_t E_{ij} E_{ij} - \rho\varepsilon \tag{8}$$

$$\frac{\partial \rho \varepsilon u_i}{\partial x_i} = \frac{\partial}{\partial x_j}\left(\frac{\mu_t}{\sigma_\varepsilon}\frac{\partial \varepsilon}{\partial x_j}\right) + C_{1\varepsilon}\frac{\varepsilon}{k} 2\mu_t E_{ij} E_{ij} - C_{2\varepsilon}\rho\frac{\varepsilon^2}{k} \tag{9}$$

Equations (8) and (9) were solved to determine turbulent viscosity,$\mu_t = \rho C_\mu k^2/\varepsilon$ for the closure of Eq. (7) where $\mu_{\text{eff}} = \mu + \mu_t$, which resolves the mean ($\bar{u}$) and fluctuation (u') in velocity.

Having established a steady-state velocity field in the domain, RTD could then be obtained by simulating the transport with a tracer under its influence. For small quantity of NaCl- or $KMnO_4$-based tracers introduced to aqueous models, the resultant change in bulk properties

Table 3 Evaluating turbulence treatment, discretization and assumption of symmetry based on final RTD parameters

Domain	Elements	Turbulence model	Location	θ_{min}	θ_{peak}	θ_{av}	V_d	V_{dp}	V_m
Full tundish	300,000	Realizable k–ε	Strand 1	0.0106	0.0218	0.6758	0.314	0.017	0.668
			Strand 2	0.0114	0.023	0.6856	0.324	0.016	0.659
			Overall	0.011	0.0224	0.6806	0.319	0.016	0.663
	152,000		Overall	0.011	0.0223	0.6807	0.319	0.016	0.664
		Standard k–ε	Overall	0.0117	0.0235	0.6839	0.316	0.017	0.666
Half tundish	109,000		Strand	0.0117	0.0234	0.6839	0.316	0.017	0.666

Table 4 Volume parameter's comparison of simulations and physical measurements in a three-strand industrial tundish [2]

Case	Simulation			Experiments		
	V_d	V_{dp}	V_m	V_d	V_{dp}	V_m
Original tundish	0.282	0.066	0.652	0.323	0.069	0.608
Modified tundish	0.222	0.191	0.588	0.498	0.091	0.411

like mass diffusivity was found to be insignificant. This effectively means that the tracer species may be modeled to be structurally similar to the bulk fluid. A pulse of tracer lasting 2 s was introduced at the inlet and its movement was tracked over time across the domain. The transient equation for transport of a non-reacting species' concentration c is given by:

$$\frac{\partial c}{\partial t} + u \cdot \nabla c = D\nabla^2 c \tag{10}$$

The system of Eqs. (6–10) was solved for multiple combinations of tundish and turbostop designs to evaluate the influence of the device on turbulence inhibition and the specificity of its performance with respect to bulk flow characteristics of the tundish, which has a lot of diversity due to variety of reservoir shape, aspect ratio, and single- or multi-strand downstream casting assemblies. This aspect of variety of tundish design was accounted for by considering three distinct reservoir designs of double-strand tundish, whose detailed floor geometries are illustrated in Fig. 1. Relevant process variables and dimensional parameters are summarized in Table 1. The design of a 7-tonne double-strand delta-shaped industrial tundish was used as the geometric basis for 1:1 scale water model simulation. The other two geometries were designed to satisfy two key features of equivalence to the delta tundish [1]:

(a) similar volumetric capacity of the tundish; and
(b) comparable geometric location of inlet and outlet.

The three bare tundish configurations were inlayed with different turbostop designs, designed to enclose comparable volume of fluid. The features of these turbostop designs are readily identifiable, in the subsequent discussion, through a three-letter nomenclature, presented in Table 2. The first character describes the state of wall inclination of turbostop, the second denotes the cross-sectional layout, and an optional third character indicates additional modifications to the device, if any.

2.2 Solution Procedure and Boundary Conditions

Single-phase calculations were performed with water. The free surface of the bath was assumed as flat and mobile [2]. There was no slip at the walls. An average cross-sectional velocity was declared at the inlet while the flow at the

Table 5 RTD and volume fraction parameters for VR of various heights in delta tundish

Design	Height (m)	θ_{min}	θ_{peak}	θ_{ave}	V_d	V_{dp}	V_m
VR	0.22	0.09	0.19	0.72	0.28	0.14	0.58
	0.11	0.09	0.18	0.72	0.27	0.13	0.59

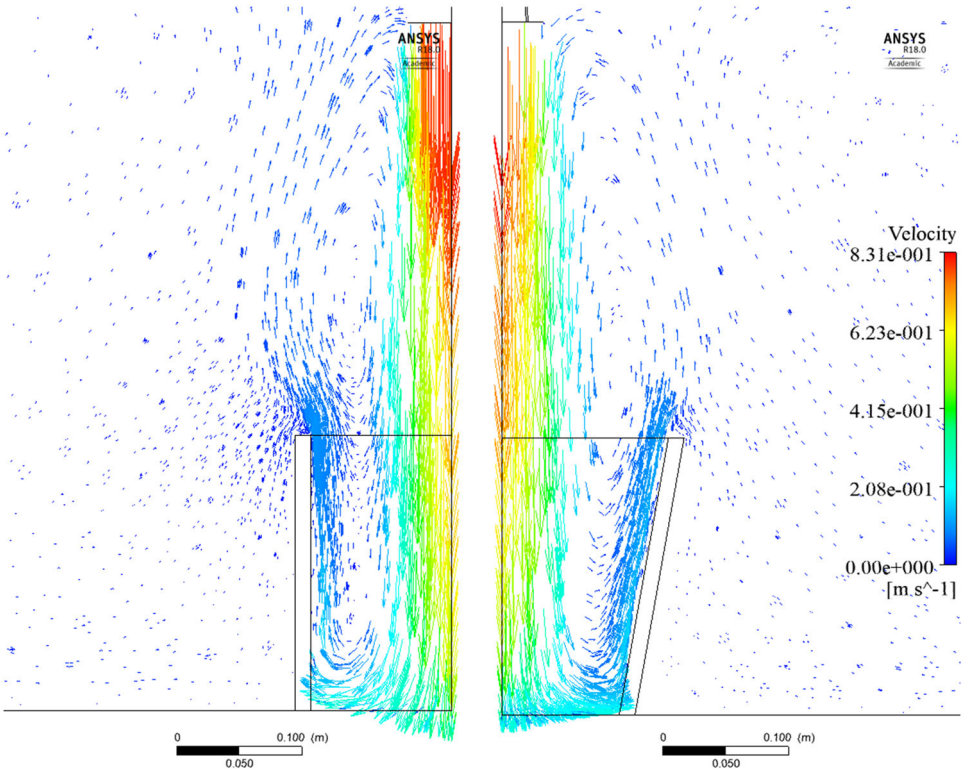

Fig. 2 Schematic vectors of redirected velocity field in vicinity of vertical *vs* tapered turbostop wall

outlet developed by virtue of hydrodynamic pressure gradient, driven by gravitational potential.

SIMPLE scheme was adopted to achieve pressure–velocity coupling [15]. Second-order upwind schemes were adopted for discretizing the equations of flow and turbulence. Grid sensitivity tests carried out in a bare delta tundish (i.e., sans turbostop) were used to determine suitable domain resolution, while ensuring desirable parameters of mesh quality such as low skewness and high orthogonality in cells [16]. Convergence criterion for solutions was set at 5×10^{-4} for all variables. Calculations were carried out using commercial solver ANSYS Fluent^{TM} 18.

3 Results and Discussion

3.1 Methodology

In order to establish a robust numerical model in the present context, two key aspects require attention:

(a) solution consistency and independence from structure of space–time discretization; and
(b) appropriate representation of symmetry in physical twin-strand tundish systems.

For the purpose of evaluating solution methodology, RTD and volume fraction parameters for bare configuration of delta tundish, obtained under variations in grid refinement, imposed symmetry and turbulence treatment, are summarized in Table 3.

There, it may be observed that the steady-state flow and consequent RTD characteristics are only nominally affected by the choice of variants of k–ε turbulence model [14, 17]. Although the realizable model is advantageous on grounds of theoretical robustness, the standard model with coefficients proposed by Launder and Spalding [14] has been adopted to simulate turbulence in the domain, on account of comparable results and smaller time to convergence.

Moreover, compared to the fine-discretized full tundish, a half-tundish domain, with artificially imposed symmetry along a transverse plane through the inlet, produces remarkably similar flow characteristics. Consequently, the half-tundish domains are used to simulate and analyze RTD characteristics in various configurations, in order to maximize grid refinement while circumventing the duplicity of calculations in symmetric full tundish.

The methodology so described was, in a related study, used to evaluate performance of three-strand industrial tundish [2]. As shown in Table 4 therefrom, residence characteristics of simulated system bear remarkable correspondence to physical measurements, indicating their suitability toward making significant scientific commentary on the physical flow phenomena. However, it must be borne in mind that even so, the simulations inherit the

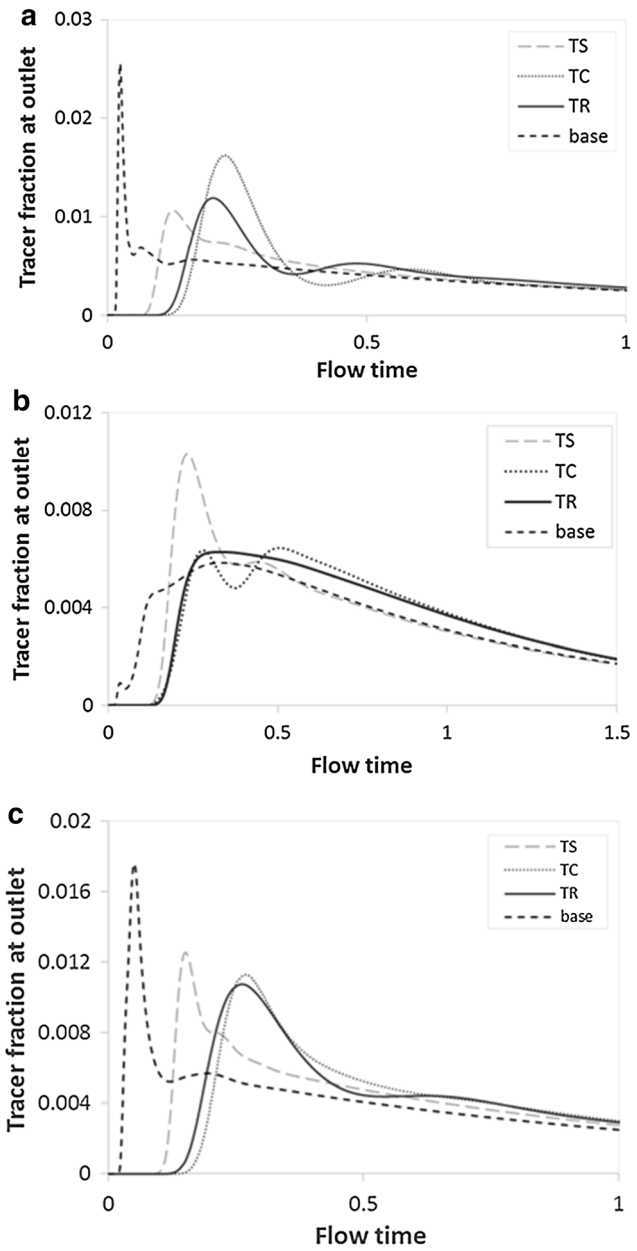

Fig. 3 Comparison of specificity of turbostop design to bulk tundish **a** delta, **b** T shaped, **c** rectangular

drawbacks of isothermal nature of water modeling, when scaling the system to capture dynamics of industrial continuous casting tundish systems, where heat flow and thermal convection hold considerable importance.

3.2 Structural Efficiency of Turbostop and Specificity to Bulk Flow in the Tundish

The distinctive difference in tundish designs is inherited by the generated flow and resultant residence time behavior. It is therefore to be expected that they will interact uniquely with the various turbostop designs, as is readily evident in the subsequent discussion. However, inferences on the underlying effect of turbostop design can be deduced from a comparative analysis of these tundish–turbostop couplings.

Analyzing the structural elements of a turbostop reveals insight on the working principle behind the device. When comparing dispersed plug flow volume, it is evident that turbostops designed with tapered walls perform better than their straight-walled counterparts, releasing flow conducive to inclusion floatation. Compared to the straight-walled design, the inclined walls offer two differentiations in its influence: the angle of deflection of the incoming stream; and the lateral surface area to offer frictional resistance. As shown in Table 5, a substantial change in surface area (50%), obtained by changing the height of turbostop, leads to nominal effect on overall flow characteristics.

Instead, the observation concurs to the idea that interactions between the fluid and turbostop occurring near the bottom of containment volume largely define the behavior of redirected jet and its subsequent evolution in the tundish bulk. This is also supported by velocity vector fields in Fig. 2, where a constricted, straight-walled geometry is seen prone to ingression, recirculation eddies and mixing of impinging and rising streams, while a tapered turbostop is able to bypass these problems by allowing for expansive rise of the redirected stream. This also underscores the importance of jet impact area in defining the size of turbostop in order to effectively redirect the stream, which is expected to show notably smaller in impingement depth and more buoyant behavior with gas–liquid shroud jet as compared to an unmixed liquid [2].

A comparison between cross-sectional layouts, involving a circular, rectangular or bulk-similar layout, reveals that designs with bulk-similar geometry, i.e., with a containment volume geometrically similar to the bulk reservoir, exhibit significantly poorer performance compared to their simpler rectangular and circular counterpart. The emergent flow from a circular cross section outperforms the other, more complicated designs, irrespective of the tundish in which they are deployed, as shown in Fig. 3. The presence of these trends across tundish designs indicates a universal favorability of structural similarity between containment volume to the incoming jet's symmetry, towards improved device efficiency. Similarity or correlation to the reservoir shape, on the other hand, appears to hold little significance toward efficiency of the device.

3.3 Influence of Terrain Modification

Projections [10] added to the turbostop wall stem from the philosophy of active retardation through increased wall friction and introducing smaller length scales, potentially expedite turbulent energy dissipation by triggering

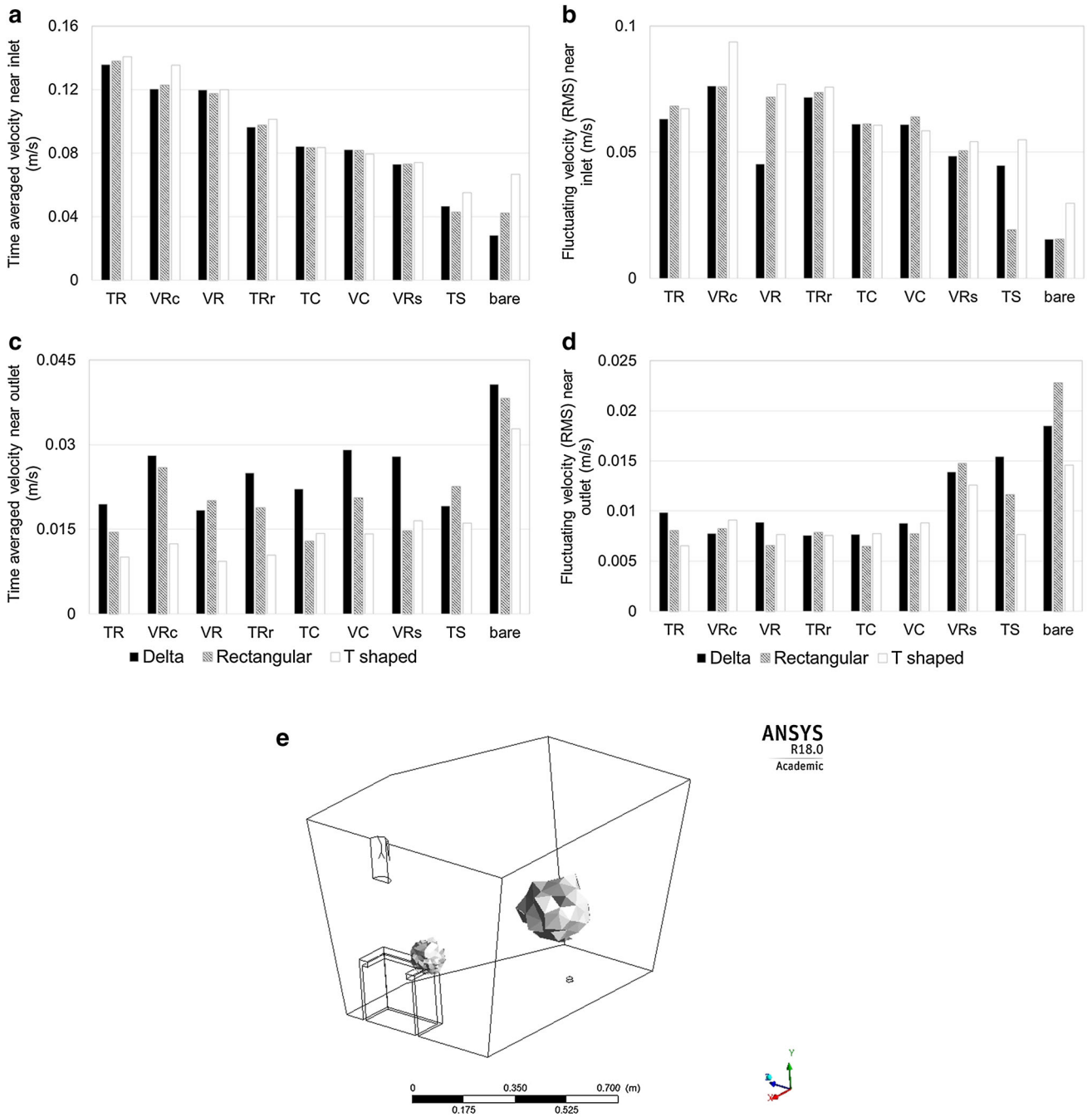

Fig. 4 Mean and fluctuating velocity components **a**, **b** in vicinity of the turbostop, and **c**, **d** in bulk flow region near the outlet, and **e** illustrative locations of sampled volume in delta tundish

multiscale turbulent cascade within the containment volume. Typical examples of such modifications are partial cover over the turbostop opening or ridges set into the wall intervals to interfere with the rising flow. VRc incorporates the former, and TRr, the latter of these.

Local regions with low turbulence kinetic energy, k are observed close to the turbostop. The resultant effect of turbulence inhibition can be examined through the time-averaged and fluctuating (as RMS) components of velocity. The k–ε model treats turbulence isotropically, so that the RMS magnitude of fluctuating velocity is derived as:

$$\langle u' \rangle = \sqrt{2k/3} \tag{11}$$

The turbulence inhibition and velocity retardation from a turbostop can be evaluated through representative velocity values near the turbostop-inlet region as well as in the bulk. Figure 4 presents the same across different

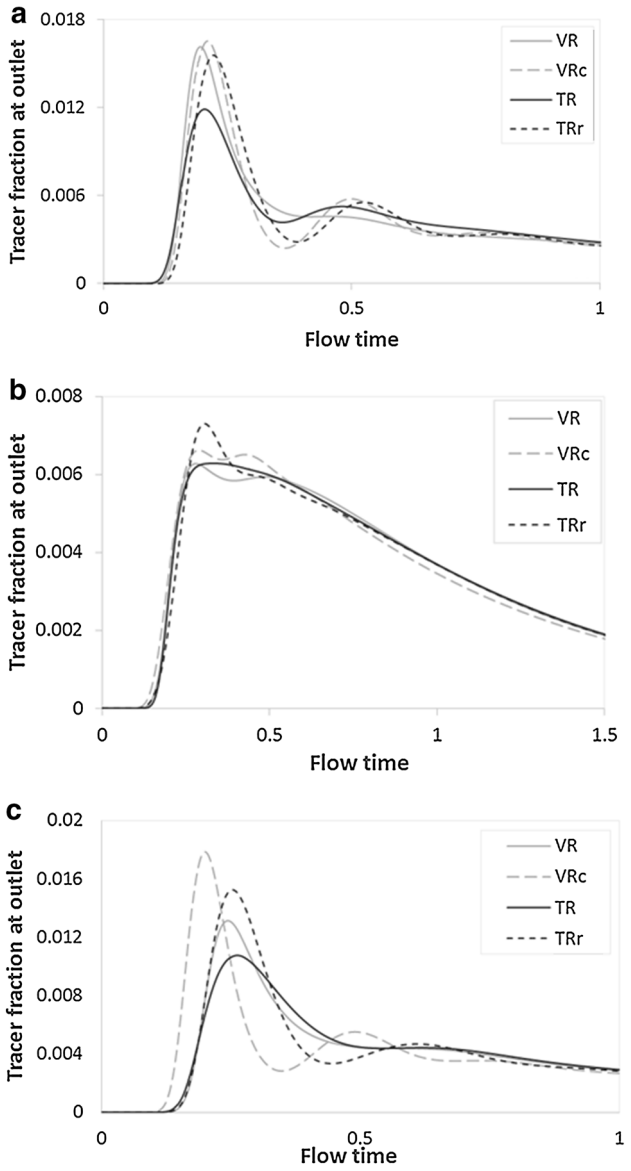

Fig. 5 Effect of modifying turbostop wall terrain on the overall flow characteristics of the tundish **a** delta, **b** T shaped, **c** rectangular

configurations, sampled from volume in the inlet (a, b) and outlet region (c, d), respectively.

Therein, a significant reduction in bulk velocity and turbulence is readily evident on the deployment of turbostop. As expected, addition of features like partial cover (VRc), or ridged interior (TRr) does generate significant turbulent energy losses in the containment volume, along with some degree of active flow retardation. The turbulent effects in the bulk, however, remain largely unaffected by this local behavior. Instead, a contained and upward directed jet results in similar quiescence in bulk of the tundish.

From an operational point of view, therefore, the influence over bulk flow and residence time characteristics appears to be marginal and not necessarily universally favorable, as shown in Fig. 5. However, evaluation of these designs in multiphase slag–metal–air systems can generate critical insights toward their efficiency in minimizing melt reoxidation around the inlet due to atmospheric exposure, since the size of exposed site will be a direct function of rise velocity [2].

3.4 Bulk Flow Agitation Through Slotted Walls

The inherent concept of turbostop and pouring boxes involves dominant redirection of the flow toward the upper region of the tundish and maximize the flotation through slag–metal interaction, while the lower strata of fluid supply clean steel to the strands, shielded from direct interaction with the incoming stream. This mechanism is often further supported by incorporation of dams and baffles in the tundish.

The addition of slots into walls of the device induces significant agitation in the lower region from the partial release of high-velocity stream, increasing the mixing near the tundish bottom. This can potentially improve coalescence and separation of smaller inclusions (less than 40 μm) which do not naturally float up to the melt-slag interface due to low buoyancy [1].

However, the orientation of these released streams is important since they drive the flow in their vicinity. The impact of relative orientation of slots is illustrated by the interaction of the three tundish geometries with the slotted rectangular turbostop VRs, containing slots near the bottom of its four walls. The flow behavior under the influence of the orientation of these slots is illustrated in Fig. 6. In each of the tundish designs, the slots release the turbulent stream partially with different orientation toward the outlet: In the rectangular tundish, the released flow is aligned directly toward the outlet while in the delta tundish, the orientation is only weakly aligned. The T-shaped tundish incorporates a redirected flow oriented away from the outlet.

Both the former designs exhibit significant tendency of short-circuiting, which is improved in the T-shaped tundish due to controlled misalignment of turbulent stream (see also Table 4). In the direct context of inclusion flotation, plug flow volume in the tundish undergoes significant deterioration under the influence of the disruptive high-velocity stream released through the slot.

Considering the increased agitation in melt bottom and the possibility of contaminating the clean melt, dispersion of ladle stream through slots cannot be recommended. Instead, introduction of properly oriented slots into devices like dams minimizes intermixing of high- and low-grade melts while also promoting inclusion coalescence near tundish bottom. Such a setup incorporating slotted dams along with a turbostop has been found to improve inclusion

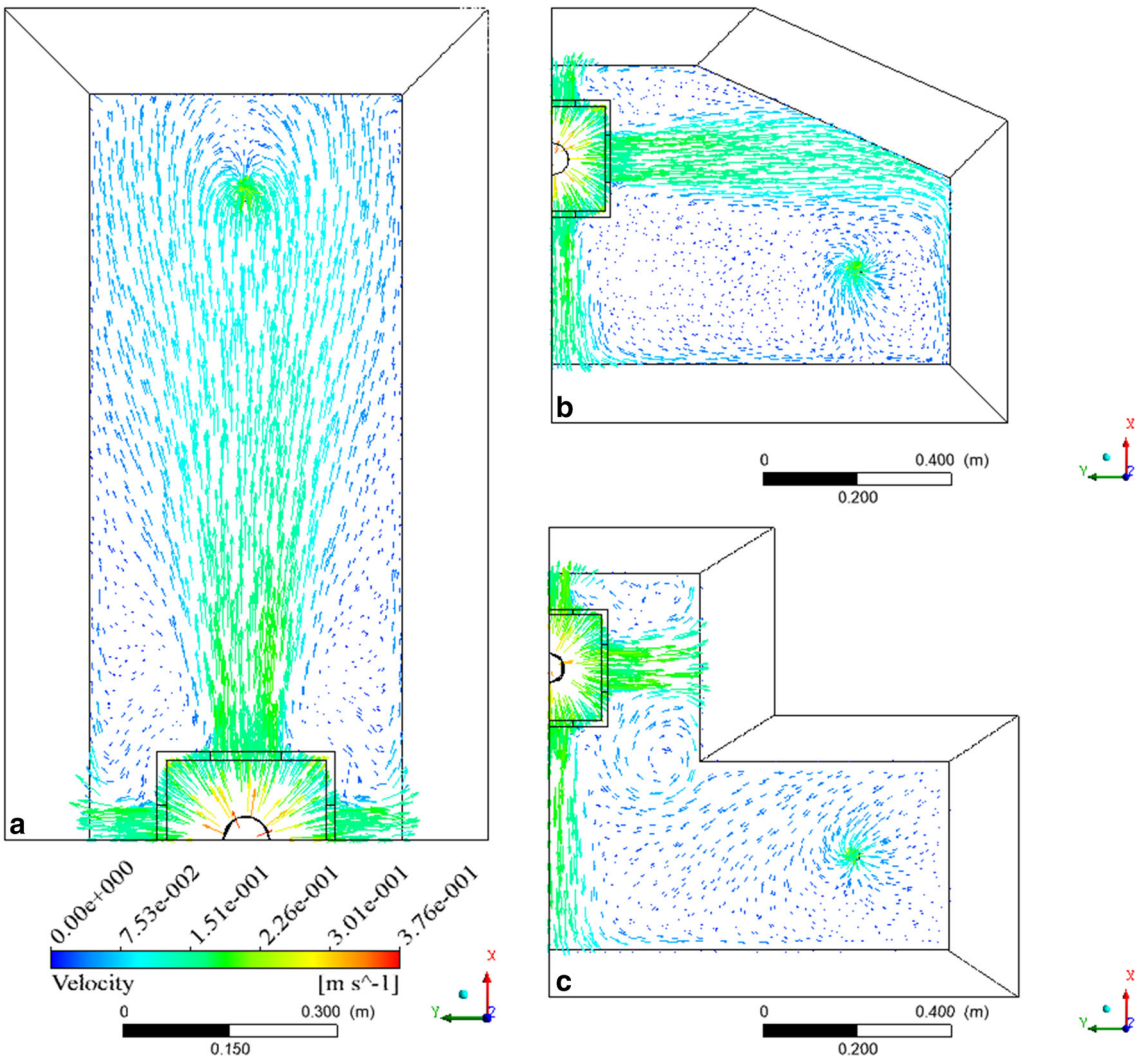

Fig. 6 Velocity vectors in the presence of slot **a** directly toward the outlet, **b** partially toward the outlet and **c** away from the outlet

flotation in a three-strand industrial tundish system, in a related investigation [2, 18].

4 Conclusion

Upon comparison of a variety of turbostop designs, employed into distinct tundish geometries, it can be concluded that an expanding, tapered device results in bulk flow in the tundish which is better suited for inclusion separation compared to the traditionally employed straight-walled design. Incorporating this element of design into simple geometries like circular or rectangular devices generates favorable flow fields, laying emphasis on the efficiency of a containment volume with resemblance to the local hydrodynamic symmetry around the shroud jet. Additional terrain modifications such as cover or ridges in the interior do not exhibit substantial and consistent improvements to the overall flow behavior. Moreover, their influence is largely limited to the inlet region. Significant insights on their desirability may be revealed upon consideration of slag displacement and steel reoxidation under the influence of the buoyant plume hydrodynamics.

References

1. Mazumdar D, and Guthrie R, *ISIJ Int* **39** (1999) 524.
2. Mishra R, and Mazumdar D, *International Conference Clean Steel*, OMBKE, Budapest (2018).
3. Sahai Y, and Emi T, *ISIJ Int* **36** (1996) 1166.
4. Palafox-Ramos J, Barreto JDJ, Lopez-Ramırez S, and Morales R, *Ironmak Steelmak* **28** (2001) 101.
5. Crowley R, Lawson G, Jardine B, and Grosjean J, *Revue de Métallurgie* **93** (1996) 967.
6. Ma T, Li H, Wang X, and Liu GQ, *Adv Mater Res* **1088** (2015) 788.

7. Schwarze R, Haubold D, and Kratzsch C, *Ironmak Steelmak* **42** (2015) 148.
8. Morales R, Lopez-Ramirez S, Palafox-Ramos J, and Zacharias D, *ISIJ Int* **39** (1999) 455.
9. Zhong L, Li B, Zhu Y, Wang R, Wang W, and Zhang X, *ISIJ Int* **47** (2007) 88.
10. Bhattacharya T, U.S. Patent No. 9,308,581 B2. Washington, DC: U.S. Patent and Trademark Office (2016).
11. Singh R, Paul A, and Ray A, *ISHMT-ASME Heat and Mass Transfer Conference*, IIT Guwahati (2006), p 2135.
12. Vasillicos A, U.S. Patent No. 5,160,480, Washington, DC: U.S. Patent and Trademark Office (1991).
13. Sharma R, and Mazumdar D, *Proceedings of the International Conference on Science and Technology Ironmaking Steelmaking*, STIS, IIT Kanpur (2017), p 371.
14. Launder B, and Spalding D, *Lectures in Mathematical Models of Turbulence*, Academic Press, New York (1972).
15. Patankar S, *Numer Heat Trans* **4** (1981) 409.
16. ANSYS Fluent 18.0 Theory Guide, ANSYS Inc., Canonsburg.
17. Shih T, Liou W, Shabbir A, Yang Z, and Zhu J, *Comput Fluids* **24** (1995) 227.
18. Kumar A, Mazumdar D, and Koria S, *ISIJ Int* **48** (2008) 38.